Purdue University
Purdue e-Pubs

International Compressor Engineering Conference

School of Mechanical Engineering

1988

On the Superior Dynamic Behavior of a Variable Rotating Speed Scroll Compressor

Noriski Ishii
Osaka Electro-Communication University

Manabu Sakai
Osaka Electro-Communication University

Michio Yamarnura
Matsushita Electric Industrial Co. Ltd. (Panasonic)

Hiroshi Morokoshi
Matsushita Electric Industrial Co. Ltd. (Panasonic)

Masafumi Fukushima
Matsushita Electric Industrial Co. Ltd. (Panasonic)

See next page for additional authors

Authors
Noriski Ishii, Manabu Sakai, Michio Yamarnura, Hiroshi Morokoshi, Masafumi Fukushima, and Shuuichi Yamamoto

ON THE SUPERIOR DYNAMIC BEHAVIOR OF A VARIABLE ROTATING SPEED SCROLL COMPRESSOR

by Noriaki Ishii[1], Michio Yamamura[2], Hiroshi Morokoshi[3], Masafumi Fukushima[4], Shuuichi Yamamoto[5] and Manabu Sakai[6]

[1] Professor, Faculty of Engineering, Osaka Electro-Communication University, Neyagawa, Osaka 572, JAPAN
[2] Director, Air Conditioning Research Laboratory
[3] Research Engineer, Air Conditioning Research Laboratory
[4] Chief Engineer, Compressor Division
[5] Engineer, Air Conditioning Research Laboratory
Matsushita Electric Industrial Co. Ltd. (PANASONIC), Noji-chou, Kusatsu 525, JAPAN
[6] Student, Faculty of Engineering, Osaka Electro-Communication University

ABSTRACT

This study compares the calculated results for the dynamic behavior of a comparatively small cooling-capacity variable-speed scroll compressor with those of a variable-speed rolling-piston rotary compressor of the same cooling capacity. The superior dynamic behavior of the scroll compressor could thus be shown. In order to derive the characteristic of the rotating speed, the rotating-speed fluctuation ratio and the rotatory acceleration, first, the equation of motion of the rotating crankshaft is solved numerically for different mean rotating speeds. Thus, the unbalanced forces of inertia exciting the whole compressor are calculated and the vibration characteristics of the compressor can be shown. In the numerical calculation, the driving torque, the gas-compression load, the frictional coefficients, the mass and the moment of inertia of the compressors are kept constant, thus the calculated results for the two different compressors can be compared.

INTRODUCTION

In recent years, many domestic electrical appliances with an inverter system has come into use. The inverter system is a device which converts a commercial alternating current into one with adjustable frequency and voltage. The inverter system is also used in air-conditioning systems to adjust the mean rotating speed of the compressors driven by the induction motor, and thus an air-conditioning system with variable speed compressor is formed. In the conventional air-conditioning systems, the compressors are operated with a constant mean rotating speed and thus the motor is switched off and on to regulate the quantity of cool air which is required for keeping the room temperature at a desired value. The switching off and on of the motor may be accompanied by large-amplitude vibrations of the compressor. As a result, the compressor hits the enclosing housing to make the noisy impulsive sounds in the reciprocating compressors [see Refs. 1-6], and in the rolling-piston rotary compressors [7] it also induces large amplitude vibrations of the pipes and panels surrounding the compressor [8]. The variable speed air-conditioning system has no vibration problems such as those which occur in compressors with constant speed operation, since the variable speed compressor can deliver the optimum quantity of cool air by adjusting the mean speed of operation,

NOMENCLATURE

e=rotating radius of rolling piston
f_{ti}=frictional force at thrust bearing
f_{xi}, f_{yi}=frictional force at Oldham ring
$[F]$=exciting force matrix
F_r=radial gas force
F_t=tangential gas force
F_{ti}=thrust force on thrust bearing
i=integer
I_c,I_o=moment of inertia of crankshaft
I_p=moment of inertia of rolling piston
I_x,I_y,I_z=moment of inertia of compressor
$[K]$=spring coefficient matrix
L_Q=frictional torque at crankshaft
L_S=frictional torque ar crankpin
l_o=height of Oldham ring
m_o=mass of Oldham ring
m_p=mass of orbiting scroll
m_v=mass of blade
$[M]$=mass matrix
N=motor torque
O_i=reaction force between Oldham ring and orbiting scroll
p_1,p_2,p_c=compressed gas pressure
p_s,p_0,p_d=suction and discharge pressure
Q_x,Q_y=reaction force on crankshaft
r_o=orbiting radius
r_Q,r_S=radius of crankshaft and crankpin
S_x,S_y=reaction force on crankpin
t=scroll thickness
T_i=reaction force between Oldham ring and fixed guide slot
x,y,z=static rectangular coordinate
x_m,y_m=orbiting coordinate
x_v=coordinate of reciprocating blade
$[X]$=displacement matrix of compressor
α=rotating-speed fluctuation ratio
β=ratio of tangetial acc. and centrifugail one
$[\gamma]$=damping coefficient matrix
θ=crank angle
θ=rotating mean speed of crankshaft
Θ_z=rotation around z axis of compressor
η_o=viscosity coefficient of oil
μ_o=frictional coefficient at Oldham ring
μ_Q=frictional coefficient at crankshaft
μ_S=frictional coefficient at crankpin

without switching the motor off and on. In addition to this point, the variable air-conditioning system has the following advantages: The energy loss in a variable speed air-conditioning system is much less than the switching-on and -off system, and thus it may be said that the variable speed system is an energy-saving system. Furthermore, the variable speed system makes it possible to control the room temperature quickly, for instance, by operating the compressor at a higher speed initially.

The variable speed type air-conditioners began to be produced in 1981 and at present about 50 % of the 2 million heat-pump type air-conditioners on the Japanese market is the variable speed type. This percentage will increase more in the future because of the variable speed air-conditioning system's great advantages. However, it should be noticed that the variable-speed type also has a tendency to induce the following vibration problem. The vibration amplitude of displacement is inversely proportional to the vibration frequency, and hence the compressor vibration displacement will increase as the operat-ing speed decreases. Moreover, the operating speed comes closer to the natural fre-quencies of the compressor supporting system, and thus the amplitude of compressor vibration has a tendency to increase due to a resonance effect. These considerations suggest that ***the scroll compressors with low-level vibration characteristics will be most suitable for the variable speed air-conditioning system.*** The scroll compressor has many compression chambers which are simultaneously compressed at comparatively low speed. Thus, the unbalanced moment of inertia about the rotating shaft is fairly small compared with that of the rolling-piston rotary compressor. Therefore, the scroll compressor will be far superior with regard to vibration than the rolling-piston rotary compressor .

Previous studies [9-11] have discussed the superior dynamic behavior of a constant speed scroll compressor. In this study, the dynamic behavior of a variable speed scroll compressor having a small cooling capacity is calculated numerically. Thus, the calculated results of the fluctuating crankshaft speed, the rotating speed fluctuation ratio, the crankshaft rotatory acceleration, the unbalanced forces and moments of inertia and the vibration displacements and accelerations are compared with those of a rolling-piston rotary compressor having the same cooling capacity. In the numerical calculation, the driving torque, the gas-compression load, the frictional coefficients, the mass and the moment of inertia of the compressors are kept constant, in order to compare the calculated results for the two different compressors.

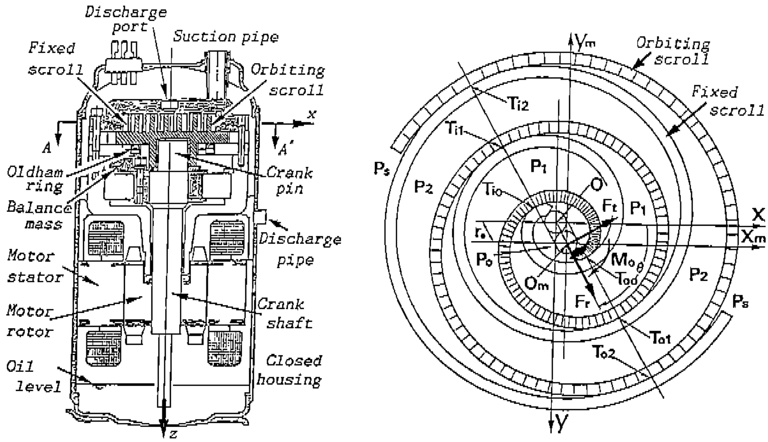

(a) Vertical cross-sectional view (b) A-A' cross-sectional view

Fig.1 Scroll Compressor

EQUATION OF MOTION AND UNBALANCED FORCES OF INERTIA

Scroll Compressor

The vertical cross-sectional view of a scroll compressor is shown in Fig. 1a. The compression mechanism is above the motor. The *A-A'* cross-sectional view of the compression mechanism is shown in Fig. 1b, in which the mating of the two identical scrolls formed by the involutes with the basic-circle radius r_b can be seen. The unshaded scroll is fixed. The basic circle center O of the fixed scroll is the origin of the static *x-y* coordinate. z is the downward axis along the crankshaft center. The shaded scroll can move in the x direction, relatively to the Oldham ring which can move in the y direction along a fixed guide slot. Thus, the shaded scroll orbits when the basic-circle center O_m of the shaded scroll rotates around the fixed point O. The orbiting radius r_o is given by $(r_b\pi-t)$ where t is the scroll thickness. The clockwise orbiting angle from the x axis is represented by θ. The contact points T_{ik} and T_{ok} $(k=0,1,2...)$ appear respectively on the two tangents common to the two basic circles. The two scrolls form a series of crescent-shaped compression chambers. The pressures p_s, p_1, p_2 and p_0 acting on the orbiting scroll are reduced to the tangential force F_t which acts against the clockwise orbiting motion, the radial force F_r and the clockwise moment M_o which act on the orbiting scroll center O_m. They are given by (4)-(6) in the previous study [9]. When the crankshaft is driven by the motor torque N, the equation of motion of the rotating crankshaft is given by the following [9, 11]:

$$(I_0+m_s r_0^2+m_o r_0^2 \sin^2\theta)\ddot{\theta} + m_o r_0^2 \sin\theta\cdot\cos\theta\cdot\dot{\theta}^2$$
$$= N-\{F_t r_0+L_Q+L_S+(f_{x1}+f_{x2}) r_0 \sin\theta + (f_{y1}+f_{y2}) r_0 \cos\theta + (f_{t1}+f_{t2}) r_0\} \quad (1)$$

where I_o is the moment of inertia of the crankshaft system comprising the motor rotor, m_s the mass of the orbiting scroll and m_o the mass of the Oldham ring. L_Q and L_S are the frictional torques on the crankshaft and the crankpin, respectively. f_{xi} and f_{yi} $(i=1,2)$ are the frictional forces acting on the Oldham ring. The subscripts x and y represent the directions of the frictional forces. f_{ti} $(i=1,2)$ are the frictional forces at the thrust bearing. They are given by the following expressions, assuming Coulomb's law of friction.

$$L_Q=\mu_Q\sqrt{Q_x^2+Q_y^2}\cdot r_Q, \quad L_S=\mu_S\sqrt{S_x^2+S_y^2}\cdot r_S$$
$$f_{xi}=\mu_o|T_i|, \quad f_{yi}=\mu_o|O_i|, \quad f_{ti}=\mu_t|F_{ti}|, \quad (i=1,2) \quad (2)$$

where Q_x, Q_y are the reaction forces on the crankshaft, S_x, S_y those on the crankpin, T_i $(i=1,2)$ those between the Oldham ring and the fixed guide slot and O_i $(i=1,2)$ those be tween the orbiting scroll and the Oldham ring. They can be easily derived from the previous study [9]. These reaction forces include the frictional forces of (2) and hence an iterative calculation method should be adopted for calculating the frictional forces and torques of (2). F_{ti} *(i=1,2)* are the reaction forces on the thrust bearing and are given by (18) in the previous study [9].

The forces and moments exciting the compressor vibrations are given by the following expressions, namely, unbalanced forces and moments of inertia:

$$F_x=-(m_o/2)r_o(\dot{\theta}^2\cos\theta+\ddot{\theta}\sin\theta),\quad F_y=-(m_o/2)r_o(\dot{\theta}^2\sin\theta-\ddot{\theta}\cos\theta),\quad F_z=0,$$
$$M_x=(m_o/2)l_o r_o(\dot{\theta}^2\sin\theta-\ddot{\theta}\cos\theta),\quad M_y=(m_o/2)l_o r_o(\dot{\theta}^2\cos\theta+\ddot{\theta}\sin\theta),\qquad (3)$$
$$M_z=-(I_o+m_s r_o^2)\ddot{\theta}$$

in which the best static balancing and the best dynamic balancing have been achieved by choosing optimum values of the balancing masses. However, as shown in Fig.1a, the orbiting scroll is supported from the bottom only, and hence the perfect dynamic balancing cannot be achieved. F_x, F_y and F_z are the forces acting on the fixed-coordinate origin *O*. M_x, M_y and M_z are moments around the *x*, *y* and *z*-axes respectively.

Rolling-Piston Rotary Compressor

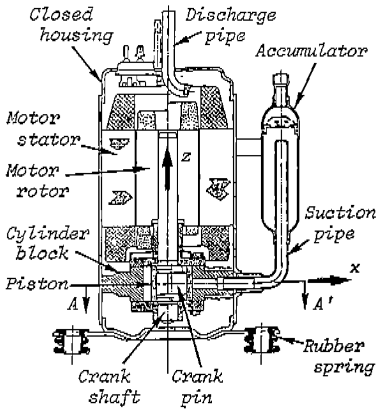

Fig.2 Rolling-piston rotary compressor

The vertical cross-sectional view of a rolling-piston rotary compressor is shown in Fig.2. A static rectangular coordinate with the origin at the cylinder center is represented by *x*, *y* and *z*-axes. *x* axis coincides with the center line of the reciprocating blade. *z* is the upward axis along the crankshaft center. The equation of motion of the rotating crankshaft has been derived in the previous study [7]. Achieving the best static and dynamic balancing, the unbalanced forces and moments of inertia are given by the following expressions.

$$F_x=-m_v\ddot{x}_v-(m_v/2)e(\dot{\theta}^2\cos\theta+\ddot{\theta}\sin\theta),$$
$$F_y=-(m_v/2)e(\dot{\theta}^2\sin\theta-\ddot{\theta}\cos\theta),\quad F_z=0,$$
$$M_x=0,\quad M_y=0,\quad M_z=-(I_c+m_p e^2)\ddot{\theta}-I_p\ddot{\varphi}\qquad (4)$$

The crankshaft is supported at both sides of the cylinder and hence the perfect dynamic balancing can be achieved. m_v and x_v represent the reciprocating-blade mass and its coordinate [see (2) of ref. 7], respectively. *e* is the rotating radius of the rolling piston with the mass m_p. I_c and I_p represent the moment of inertia of the crankshaft and the rolling piston, respectively.

NUMERICAL CALCULATIONS

Frictional coefficients

When a small cooling capacity rolling-piston rotary compressor was driven by a motor with shaft power of about *600 W*, the measured mechanical efficiency was *90.3 %* and the measured rolling-piston mean speed was 32 *rpm* under a suction pressure of 0.54 *MPa* and discharge pressure of 2.06 *MPa* [12]. On the basis of these measured values, the lubrication at each pair of machine elements in the mechanism was evaluated theoretically, by using those into three major categories of lubrication: a fluid lubrication between the rolling piston and the crankpin, a comparatively well-conditioned boundary lubrication between the crankshaft and the crank journal, and a comparatively poorly-conditioned boundary lubrication between the blade and the rolling piston or the cylinder guide slot [13]. It was concluded from this study that the frictional coefficient at the crankshaft is *0.013* and the frictional coefficient at the blade is *0.083* when the oil viscosity coefficient is about 2.076 *mPa·s*. In order to compare the calculated results for the two different compressors, it is assumed that the frictional coefficients in the scroll compressor are as follows: The frictional coefficients μ_Q and μ_S at the comparatively well-lubricated crankshaft and crankpin are *0.013*, and μ_O and μ_t at the comparatively poorly-lubricated Oldham ring and thrust bearing are *0.083*.

Motor Torque and Gas Pressure

The motor torques for five synchronous speeds from *30* to *150 Hz* are shown by dotted lines in

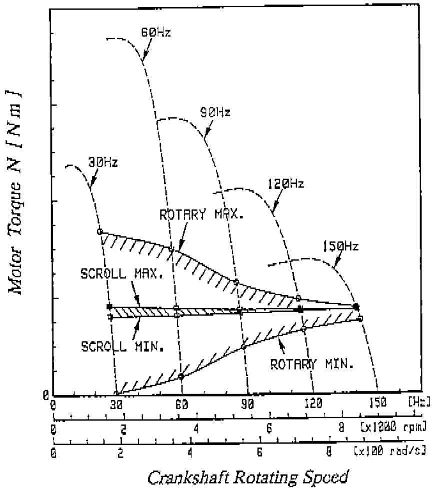

Fig.3 Motor torque and the range of torque fluctuation

Fig. 3. In the numerical calculations, these motor torque curves are approximated by a 4th-order polynomial expression for the rotating speed θ. Assuming that the gas compression process is subjected to the adiabatic change of specific heat ratio *1.32* which is the value of the superheated Freon *(R-22)* vapor at a pressure of *1.32 MPa* and a temperature of *55.6 °C,* the pressures in the compression chambers are calculated. The suction pressure is *0.617 MPa* and the discharge pressure is *2.17 MPa.*

Table 1 Major mechanical constants

Scroll Comp.	*Rotary comp.*
$I_o=0.0422$ $Ncms^2$ $m_o=0.051$ Kg $m_s=0.277$ Kg $r_o=0.25$ cm $r_Q, r_S=1.0$ cm	$e=0.326$ cm $I_c=0.0422$ $Ncms^2$ $I_p=0.0015$ $Ncms^2$ $m_p=0.0741$ Kg $m_v=0.0113$
$I_X=3.519$ $Ncms^2$ $I_Y=3.904$ $Ncms^2$ $I_Z=0.996$ $Ncms^2$ $M=8.7$ Kg $(x_G, y_G, z_G)=(6.54$ $cm,$ $0,$ $0)$	

Mechanical Constants

Table 1 shows the major mechanical constants of the two compressors having a small cooling capacity. The maximum suction volume is *10.26 cm^3*. The crankshaft moments of inertia I_O and I_C are the same. As shown in (3) and (4), the unbalanced forces and moments of inertia except for M_Z consist of the inertia terms of the reciprocating elements: the Oldham ring in the scroll compressor and the blade in the rolling-piston rotary compressor. Thus, it should be noticed that the mass m_O of the Oldham ring is about 5 times larger than the mass m_V of the blade. This difference is caused by the structural difference between the scroll compressor and the rolling-piston rotary compressor.

Calculated Results for Crankshaft Dynamic Behavior

The crankshaft dynamic behavior of the scroll compressor can be calculated numerically from the expressions (1) and (2), as follows: The initial values of θ and $\dot{\theta}$, and the crankshaft mean rotating speed which is a little smaller than the synchronous speed are given first, and thus θ, $\dot{\theta}$ and $\ddot{\theta}$ over one period are calculated. The initial value of $\dot{\theta}$ is modified if θ does not increase in one period by one revolution 2π, and the crankshaft mean rotating speed is modified if $\dot{\theta}$ after one period does not coincide with the initial value, to repeat the same numerical calculation over one period again. Thus, the periodical dynamic behavior of the crankshaft is obtained. The range of fluctuation of the motor torque is shown in *Fig.3,* in which the calculated results for the same cooling capacity rolling-piston rotary compressor are shown. The torque fluctuation of the scroll compressor is far smaller than those of the rolling-piston rotary compressor. It is evident from this character that the crankshaft rotating speed fluctuation ratio α of the scroll compressor is far smaller than the rolling-piston rotary compressor, as shown in *Fig.4.* As the synchronous speed decreases, α for both compressors increase, but the increasing ratio for the rotary compressor is far larger than the scroll compressor.

The increase of α for the decreasing synchronous speed is caused by the following character of the crankshaft rotatory acceleration $\ddot{\theta}$: *Fig.5* shows the peak to peak value of the fluctuating acceleration $\ddot{\theta}$. The peak to peak value has a tendency to decrease, as the synchronous speed decrease, but the decrease is quite small for both compressors. As seen from (1), $\ddot{\theta}$ depends mainly upon the fluctuating gas load $(F_t r_o)$ which is kept constant for each synchronous speed, and thus $\ddot{\theta}$ is fundamentally constant independently of the synchronous speed. The small decrease of $\ddot{\theta}$ for the decreasing synchronous speed is caused mainly by a decrease of frictional torques and forces which are partially af-

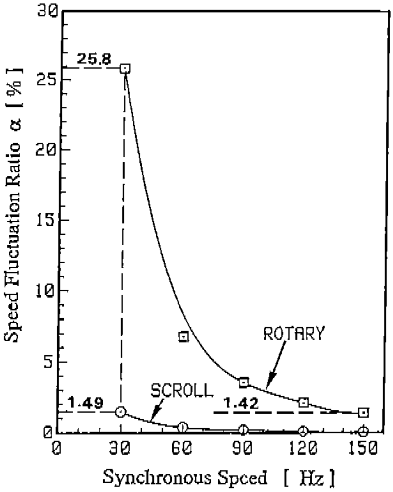

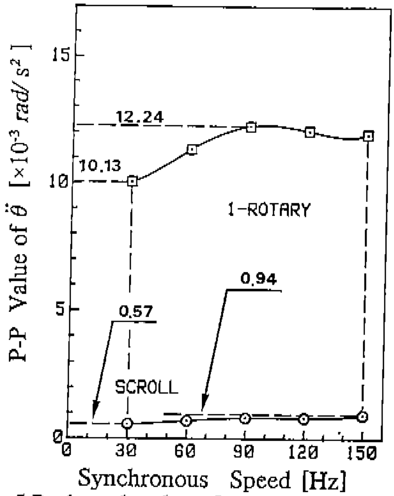

Fig.4 Crankshaft speed fluctuation ratio *Fig.5 Peak-peak value of rotatoryacceleration*

fected by the centrifugal acceleration. The centrifugal acceleration decreases, of course, as the synchronous speed decreases.

Compressor Vibration

The compressor vibration is subjected to the following matrix equation of motion:

$$[M][\ddot{X}]+[\gamma][\dot{X}]+[K][X]=[E][F] \tag{5}$$

where $[X]$ represents the displacements of the compressor gravity center, which consist of X, Y, Z, Θ_X, Θ_Y and Θ_Z. $[M]$ is the mass matrix consisted of M, I_X, I_Y and I_Z which are given in Table 1. $[\gamma]$ is the damping coefficient matrix and $[K]$ the spring constant matrix. $[E]$ is a transfer matrix which consists of the gravity coordinate x_G, y_G and z_G (see Table 1) and is given by (28) in the previous study [9]. Assume that the damping effect of coiled springs can be neglected and the undamped natural frequencies are *8.6 Hz* in the x and y directions, *15 Hz* in the z direction, *15.1 Hz* around the x axis, *11.9 Hz* around the y axis and *13.6 Hz* around the z axis. Thus, the compressor vibrations can be calculated.

As shown in (3) and (4), the unbalanced forces and moments except for M_z consist of both accelerations $\dot{\theta}^2$ and $\ddot{\theta}$. It is important to find that even when the synchronous speed is *30 Hz*, the maximum value of the centrifugal acceleration $\dot{\theta}^2$ is about *7* times larger than that of the rotatory acceleration $\ddot{\theta}$, that is, the exciting forces and moments except for M_z depend mainly upon the centrifugal forces of the unbalanced mass, which vary proportionally to the quadratic rotating speed. On the other hand, the vibration displacements vary inversely proportional to the quadratic rotating speed. Thus, the amplitude of the vibration displacements is almost constant for any synchronous speed. As an instance, the vibration displacement X_G in the x direction is shown in *Fig.6*, in which the horizontal axis is the crank angle θ. As shown in *Table 1*, the mass m_O of the Oldham ring is larger than the mass m_V of the blade. Thus, the amplitude of the scroll compressor is larger than the rolling-piston rotary compressor, but the maximum amplitude is quite small *7.37 μm*.

The most significant component of the compressor vibrations is the rotation Θ_Z around the z axis. As given by the last expressions in (3) and (4) respectively, the unbalanced moment of inertia M_z which excites the vibration Θ_Z consists mainly of the rotatory acceleration $\ddot{\theta}$. As shown in *Fig.5*, the amplitude change of the rotatory acceleration $\ddot{\theta}$ for the synchronous speed is very small compared with a change proportional to the quadratic rotating speed, that is, the exciting moment M_z is considered to be almost constant for any synchronous speed. Thus, the amplitude of the rotation Θ_Z increases inversely proportional to the decreasing quadratic synchronous speed, as shown

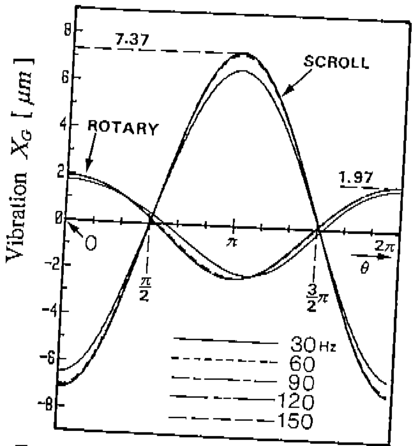

Fig.6 Vibration curves of X_G

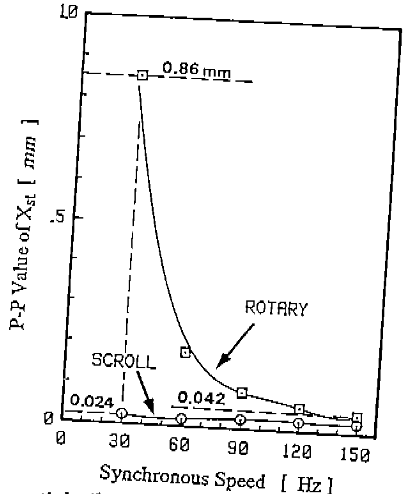

Fig.8 Tangential vibration on compressor housing

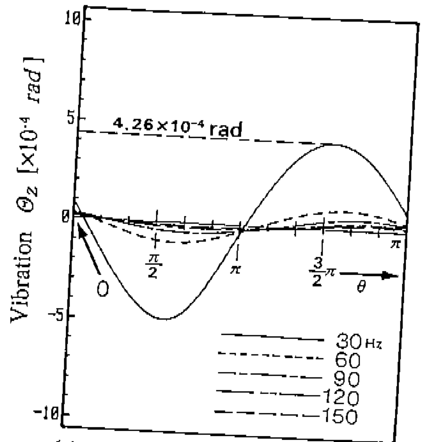

(a) Scroll Compressor

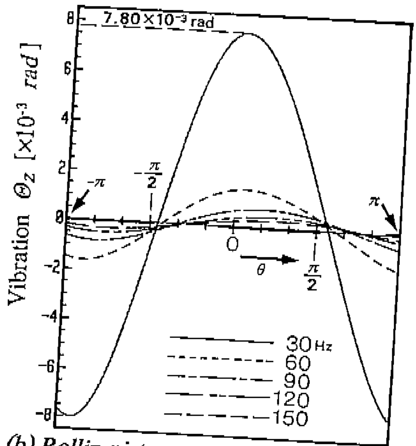

(b) Rollin-piston rotary compressor

Fig.7 Vibration curves of compressor rotation Θ_Z around z axis

in *Fig. 7*. *Fig. 7a* shows the calculated results for the scroll compressor and *Fig. 7b* those for the rolling-piston rotary compressor. Both figures show the same tendency that the rotation amplitude increases inversely proportional to the quadratic synchronous speed. However, the rotation amplitude of the scroll compressor is far smaller than the rolling-piston rotary compressor. The rotation amplitude of the scroll compressor at the synchronous speed *30 Hz* is quite small 4.26×10^{-4} *rad* which is about *25 dB* smaller than 7.8×10^{-3} *rad* of the rotary compressor.

The amplitude characteristics of the tangential vibration X_{st} on the compressor housing with the radius *55 mm* is shown in *Fig.8*. It is a matter of course that the main factor inducing the tangential vibration X_{st} is the rotation Θ_Z shown in *Fig.7*. Thus, as the synchronous speed decreases, the peak to peak value of X_{st} for the rolling-piston rotary compressor increase rapidly. But X_{st} for the scroll compressor is almost independent of the synchronous speed and its peak to peak value is quite small *0.024 mm* which is about *31 dB* smaller than the maximum value *0.86 mm* at the synchronous speed *30*

Hz for the rolling-piston rotary compressor.

CONCLUSIONS

The dynamic behavior of a small cooling capacity variable-speed scroll compressor with a suction volume of *10.26* cm^3 which is operated at a suction pressure of *0.617 MPa* and a discharge pressure of *2.17 MPa* was calculated for *5* different synchronous speed from *30* to *150 Hz,* and the calculated results were compared with those of a variable-speed rolling-piston rotary compressor having the same cooling capacity. It is concluded from this study that the variable speed scroll compressors have the following dynamic behavior which is far superior than the variable-speed rolling-piston rotary compressors: The crankshaft speed fluctuation ratio of the scroll compressor is very small compared with the rolling-piston rotary compressor. For instance, it is *1.49 %* at the synchronous speed *30 Hz,* which is about one seventeenth of *25.8 %* for the rolling-piston rotary compressor. The compressor vibration displacements except for the component around the rotating crankshaft have almost the same amplitude for any synchronous speed. However, the amplitude of the compressor rotation around the rotating crankshaft increases, as the synchronous speed decreases. Especially, the amplitude for the rolling-piston rotary compressor increases up to a large value which is *25 dB* larger than the scroll compressor, when the synchronous speed is *30 Hz.* As a result, the peak to peak value of the tangential vibration on the compressor housing of the scroll compressor is quite small *0.024 mm* which is about *31 dB* smaller than the rolling-piston rotary compressor, even when the compressor is driven by the motor with the synchronous speed *30 Hz.*

ACKNOWLEDGEMENT

The authors would like to express their great thanks to Mr. *Kazuhiko SUGIYAMA,* Head of Compressor Division, *Kazumasa YOSHIDA,* Head of Air Conditioner Division, *Hisao OOUCHI,* Director of Air Conditioner Division and *Nobuhisa ITOO,* Head of Air Conditioning Research Laboratory, Matsushita Electric Industrial Co. Ltd., for their financial support in carrying out this work and their permission to publish this work. They also wish to express their sincere thanks to Chief Engineers, Mr. *Yasuhiko SANO* ans Mr. *Shigeru MURAMATSU* for their help in completing this study.

REFERENCES

1. Imaichi, K., Ishii, N., et al., "Vibration of a Small Reciprocating Compressor," ASME Paper 75-DET-44, 1975, Washington, D.C..
2. Imaichi, K., Ishii, N., et al., "Leakage Effects on Indicator Diagram at Stopping of Reciprocating Compressors," Proc. the Purdue Compressor Technology Conference, July, 1978, pp.283-288.
3. Imaichi, K., Ishii, N., et al., "A Device for Stopping Single-Cylinder Reciprocating Compressors silently by Greatly Reducing Vibrations," Proc. the 15th Int. Congress of Refrigeration, Sept., 1979, pp.727-733.
4. Imaichi, K., Ishii, N., et al., "Higher Frequency Vibratory Components Caused by Elastic Vibrations of the Crank Shaft in Reciprocating Compressors," Proc. the Purdue Int. Compressor Engineering Conference, July, 1983, pp.90-96.
5. Ishii, N., et al., "A Computer Simulation of Higher Frequency Vibrations of a Reciprocating Compressor," Proc. the 16th Int. Congress of Refrigeration, Paris, Sept., 1983, pp. 418-423.
6. Imaichi, K., Ishii, N., et al., "A Vibration Source in Refrigerant Compressors," Trans. ASME: J. Vibration, Acoustics, Stress and Reliability in Design, Vol.106, 1983, pp.122-128.
7. Imaichi, K., Ishii, N., et al., "Vibration Analysis of Rotary Compressors," Proc. the Purdue Compressor Technology Conference, July, 1982, pp.275-282.
8. Ishii, N., et al., "The Study of Rolling-Piston Rotary Compressor Dynamic Behavior When Stopping to Reduce Noise and Vibration Level," Proc. the Purdue Int. Compressor Engineering Conference, July, 1984, pp.259-266.
9. Ishii, N., et al., "A Study on Dynamic Behavior of a Scroll Compressor," Proc. the Purdue Int. Compressor Engineering Conference, Vol.3, Aug., 1986, pp.901-916.
10. Ishii, N., et al., "Mechanical Efficiency of Various Large Capacity Scroll Compressors," Proc. the 17th Int. Congress of Refrigeration, Wien, Aug., 1987, pp.468-474.
11. Ishii, N., et al., "Dynamic Behavior of a Scroll Compressor (Dynamic Analysis)," JSME Int. J. (published by the Japan Society of Mechanical Engineers), Series 3, Vol.31, No.1, March, 1988, pp.58-67.
12. Ishii, N., et al., "The High Mechanical Efficiency of Rolling-Piston Rotary Compressors (1st Report, Experimental Study)," (in Japanese), to be presented at a JSME Conference on Aug., 1988.
13. Ishii, N., et al., "The High Mechanical Efficiency of Rolling-Piston Rotary Compressors (2nd Report, Theoretical Study)," (in Japanese), to be presented at a JSME Conference on Oct., 1988.